RESEARCH
www.commprac.com
ISSN 1462 2815

GREEN SYNTHESIS OF SILVER NANOPARTICLES FROM *MURRAYAKOENIGII* L. LEAF EXTRACT AND EVALUATION OF ITS ANTIDIABETIC PROPERTIES

Ashok Kumar Tripathi [1], and Jhansee Mishra [2]*

[1] Institute of Pharmacy V.B.S. Purvanchal University, Jaunpur, Uttarpradesh, India.
[2] Assistant Professor, Institute of Pharmacy V.B.S. Purvanchal University, Jaunpur, Uttarpradesh, India. *Corresponding Author Email: alokjina@gmail.com

DOI: 10.5281/zenodo.10991350

Abstract

One of the most prevalent metabolic diseases, type 2 diabetes mellitus is typified by elevated blood sugar levels brought on by either impaired insulin action or secretion, or by both. Although metformin is the most widely prescribed medication for Type 2 Diabetes Mellitus, people respond poorly and slowly to it due to its sluggish mechanism of action and numerous adverse effects. Presently, researchers are attempting to overcome these constraints through the development of nanomedicine. This study intends to clarify the therapeutic potential of silver nanoparticles as an antidiabetic medication on streptozotocin-induced diabetic BALB/c mice. It reports a unique synthesis of silver nanoparticles using MurrayaKoenigii aqueous extract. Using MurrayaKoenigii, green production of silver nanoparticles against diabetes was performed. FT-IR, SEM, TEM, and XRD were used to characterize the produced silver nanoparticles. The outcomes demonstrated that the produced particles were nanoscale in size and spherical in shape. The particles exhibit greater level antidiabetic potential, according to the investigation on their in vivo antidiabetic activities. It also displayed reduced cytotoxicity and increased antioxidant activity. The conclusion was that the greenly produced silver nanoparticles had potential as a phytomedicine to cure diabetes.

Keywords: Silver Nanoparticle, Antidiabetic Action, TEM, SEM, MurrayaKoenigii.

1. INTRODUCTION

Insulin Independent Diabetes Mellitus (IDDM), another name for Type 2 Diabetes Mellitus, is a chronic, complex illness that causes significant rates of co-morbidity worldwide [1]. In type 2 diabetes, the pancreatic β cells fail, resulting in insulinopenia and insulin resistance in the liver, skeletal muscles, and adipose tissues. This ultimately causes metabolic dysregulation and failure in these tissues [2]. The pancreas plays a vital role in controlling blood glucose levels by releasing enzymes in response to signals. According to the World Health Organization (WHO), 422 million people worldwide have diabetes, which accounted for 1.6 million deaths in 2016. This makes diabetes the seventh leading cause of morbidity and death globally. Globally, 640 million people are predicted to have diabetes by 2040 [3]. Diabetes Mellitus is thought to be caused by a variety of pathways and variables, yet the precise causes remain unknown [4]. Type 2 Diabetes Mellitus is a condition with numerous etiologies, and it is most likely caused by a genetic vulnerability exacerbated by environmental factors [5]. Diabetes mellitus manifests as polyuria (excessive urine secretion), polydipsia (excessive thirst), weariness, impaired vision, numbness in the hands and feet, weight loss, and exhaustion [6]. Dietary restrictions, weight management, and physical activity are the first lines of treatment for type 2 diabetes. Reduced glucose uptake by cells and decreased glycogen synthesis are the results of insulin resistance, which is brought on by a high calorie diet and the accumulation of extra adipose tissue [7, 8].

The physiochemical and biological processes have made substantial use of nanomaterials, which has led to a steady growth in the focus on their manufacture. Several special metals, such as copper, gold, palladium, and silver, were used to create nanoparticles. One of these metals that is commonly utilized to make nanoparticles is silver. Silver nanoparticles can be produced using a variety of methods, such as biological and physico-chemical ones. For this technology, the biological route of synthesis makes more sense because it is non-toxic and environmentally benign. Silver nanoparticles, or AgNPs, have garnered a lot of attention because of their special qualities, which include optical behavior, catalytic activity, electrical conductivity, and chemical durability. Green synthesized nanoparticles are used in the material sciences, biochemistry, and medicine. The green-produced silver nanoparticle has several medical uses due to its antioxidant [11], antidiabetic [10], and anticancer [9] characteristics. Both the compounds based on silver and the silver ions are toxic to the bacteria. They looked into how effective they were as biocide against several dangerous microbes [12]. Silver nanoparticles are used commercially in wound care, biomolecular detection, medicine administration, and diagnostic research [13–14]. Herbal-based nanomedicines are currently becoming more and more necessary in therapeutic applications [15]. Beyond glycaemic management, diabetes is a chronic illness that requires ongoing medical care and multifactorial risk-reduction strategies.[16] Developments in the knowledge of diabetes' metabolic staging have resulted in substantial improvements in the treatment plan for this debilitating condition. [17,18] Since enzymes are essential for catalyzing biochemical pathways, enzyme inhibitors are likely to be the focus of several disease prevention and treatment strategies. Controlled dynamics of monosaccharide absorption and carbohydrate assimilation may be crucial in preventing conditions including diabetes, obesity, hyperlipoproteinemia, and hyperlipidemia. α-amylase and glucosidase inhibitors are particularly important in this regard. [19,20] Preclinical investigations involving in vitro methods are essential for any activity that could potentially support in vivo studies. [21,22] Metal nanoparticles have certain characteristics that set them apart from bulk materials. The utilisation of nanoparticles for cellular delivery has become widespread due to their ability to target specific locations for medication release, high functionality, and accessibility. consequences [23, 24]. There are no published reports of the creation of green silver nanoparticles via photocatalysis using the aqueous leaf extract of MurrayaKoenigii. The current effort aimed to optimize the different parameters for an efficient green production and to characterize the silver nanoparticles using different methodologies. These nanoparticles were compared to the diabetic action of green synthetic nanoparticles in order to assess their potential as an anti-diabetic drug.

2. MATERIALS AND METHODS

2.1 Preparation of Leaf Extract

The Pharmacy Department of Veer Bahadur Singh Purvanchal University supplied freshly harvested MurrayaKoenigii leaves that had undergone double distillation for purification. Extracts of plant materials were extracted from them. Fifteen grams of pulverized leaves and one hundred milliliters of distilled water were added to the mixture. The solvent was filtered through Whatman 1 filterpaper after being heated to 100°C for two minutes in order to extricate the constituents of the leaves. It was

subsequently chilled to room temperature. Temperature control for the extracted solution was four degrees Celsius.

2.2 Synthesis of Silver Nanoparticles

The silver nanoparticles were produced utilizing the aqueous leaf extract of MurrayaKoenigii that was formulated in the preceding stage. To accomplish this, 10 mL of leaf extract was added to 90 mL of a 1 mM aqueous silver nitrate solution, which was boiled at 80 °C for three hours with constant agitation. The initial indicator of AgNPs maturation was a transition in hue from yellow to dark brown. The green nanoparticles were isolated by means of 20 minutes of centrifugation at 15,000 H g. Three repetitions of this procedure were necessary to remove the liberated silver that was linked to the Cp-AgNPs. Cp-AgNPs, the final silver nanoparticles produced via green synthesis, were freeze-dried and kept at 4 °C until they were once again needed.

2.3 Characterization of Silver Nanoparticles Synthesized in Green

2.3.1 UV-Vis Spectroscopy

To monitor the production of silver nanoparticles, the optical density of the reaction mixture was measured at various time intervals using a Shimadzu UV-1800 double beam UV–Vis spectrophotometer with Milli Q water serving as a blank. The wavelength range in which the absorbance of the reaction mixture was measured was 300–700 nm.

2.3.2 SEM Examination

Analyses by means of scanning electron microscopy (SEM) were conducted using an EVOSEM MA 15/18 coupled with an EDS instrument. A minuscule quantity of the specimen was applied onto a copper grid in order to fabricate a thin film of the substance. In order to ascertain the presence of elemental silver in AgNPs, an examination was conducted on the nanoparticles' dimensions and morphology via scanning electron microscopy (Nova Nano SEM 450, USA).

2.3.3 Analysis by TEM

To prepare the sample for analysis by transmission electron microscopy (FEI USA), the AgNPs colloidal solution was subjected to centrifugation at 10,000 rpm for 15 minutes at 25 °C. This process eliminates any non-covalently attached molecules from the structures of the AgNPs. To further assure the uniform distribution of the nanoparticles, the substance underwent additional sonication. (25)

2.3.4 XRD

Utilizing an X-ray diffractometer (Rigaku Minifex 600) outfitted with a Cu Kα radiation source and a nickel monochromator filter, the X-ray diffraction pattern (XRD) of AgNPs was analyzed. The scanning rate was set at 2° min−1. The 2θ range of 20°–80° was accounted for by the filter.

2.3.5 Fourier Transform Spectroscopy (FT IR) Analysis of Infrared

The determination of the silver nanoparticle's surface characteristics was accomplished by analyzing Fourier transform infrared (FTIR) spectra of the desiccated extract and nanoparticle through the utilization of an FTIR spectrophotometer (Bruker, Germany), within the spectral range of 4000–400 cm−1.

2.4 Research into Acute Toxicity

When required, accurately weighed test samples were immediately triturated with water and 1% CMC. For duration of 15 days, test samples were administered orally via gavage at a dosage of 100 mg/g. Upon completion, urine samples were obtained from the animals, and blood samples were procured through cardiac puncture and subsequently processed according to the specifications of the analysis.

2.5 In vivo study of anti-diabetic effectiveness using animal models

Wistar rats were housed in 25°C, 12-hour light–dark cycles, noise-controlled chambers. The animals had unrestricted access to water and were fed a standard pellet diet. Test samples were given intraperitoneally (I.P.) in accordance with body weight and precisely weighed. At the end, animal urine samples were collected, and blood samples were drawn via cardiac puncture and processed in compliance with the analysis's specifications.

2.5.1 SGOT

By moving an amino group from L aspartate to keto glutamate, SGOT catalyzes the synthesis of glutamate and oxaloacetate. The oxaloacetate that was formed when malate dehydrogenase was present mixes with NADH to form NAD. The rate of oxidation of NADH to NAD was determined by measuring the absorbance drop, which is also connected with the sample's SGOT activity.

One milliliter of enzyme and five milliliters of start reagent were mixed to create the working reagent. Following the addition of 20 ul of serum sample and 100 ul of working reagent, the OD was measured at 340 nm at 25–30C for two and a half minutes. To get the final result, the OD difference was calculated and multiplied by 952. The units of measurement were IU/L. Reagent sizes were lowered as necessary.

2.5.2 SGPT

SGPT converts L-alanine and alpha ketoglutarate into pyruvate and glutamate. A brown complex with measurable intensity was created when 2,4, Dinitrophenyl Hydrazine and Pyruvate were mixed together. In summary, we mixed 0.3 ml of substrate reagent, 0.2 ml of pyruvate standard, 0.1 ml of DW, and 0.05 ml of DNPH reagent, and then we allowed it to stand at room temperature for 20 minutes. We checked and adjusted the OD.

0.50 ml of substrate reagent was incubated at 37C for three minutes. Add the serum sample (0.1 ml). After giving it a good stir, leave it at 37°C for three minutes. Add the serum sample (0.1 ml). After fully combining, incubate at 37°C for 30 minutes. Pour in 0.5 ml of the DNPH solution. Once well combined, incubate at room temperature for 20 minutes. Add the NaOH reagent in 5 milliliters. After fully combining, let sit at room temperature for 10 minutes. At 505 nm, locate the OD. The size of the reagent was lowered as needed.

2.5.3 WBC

Put 20 ul of blood and 380 ul of WBC dilution solution into a Neubauer chamber. Count the cells in the WBC region of the chamber. A substantial area is 1 × 1 mm in size and has a 0.1 mm depth. 0.4 µL (4/10) is equal to four large squares times the total area, or 4 x 1 x o.1. Y x 10/4 is the total WBC in a single µL. It is now 1:20 dilution.

WBC count total = Y x 10 x 20/4 = Y x 50 = 1µL of cells. Total WBC - counted cells Yx 50 = WBC/cu mm.

2.5.4 RBC

Put 20 ul of blood and 3980 ul of RBC dilution solution into a Neubauer chamber. Count the cells in the WBC region of the chamber. Count the cells in the RBC region of the chamber. The amount of RBCs multiplied by 10,000 yields RBCs X106/mm. The factor to be multiplied is 10 x 200 / 0.2 = 10,000.

2.5.5 Haemoglobin

After confirming that the haemoglobin pipette and tube are dry. Add N/10 HCl until the 2g% threshold is met. Once the EDTA sample has been gently mixed, add 0.02 ml of blood to the pipette. Make sure there are no air bubbles in the pipette. Remove it and pipette again if it comes in. Wipe the outside of the pipette to remove excess blood. Once the blood has been added, fill the tube with HCl. Pull in and blow out the acid many times to wash away the contents of the hemoglobin pipette in order to thoroughly mix the blood with the acid. Allow the combination to lie motionless for ten minutes (this is because the first 10 minutes are when hemoglobin changes to acid hematin at its greatest rate). Then, slowly add distilled water to the mixture after inserting the hemoglobinometer tube into the comparator. Work the glass rod until the comparator glass and its color match. Note the result as the reading of the lower meniscus of the solution. The glass rod must be removed from the solution and held upright in the tube while keeping the same color. (Note that the stirrer must be in the solution above the level rather than out of the tube.). To express the hemoglobin content, use g/dl.

2.5.6 HCT

An HCT tube is used to centrifuge blood. The majority of RBCs will settle, and clear plasma will ascend to the top. This represents the ratio of settling cells to upper clear plasma expressed as a percentage.

2.5.7 Clotting Time

Blood collected in a capillary tube via orbital puncture. Up until a clot thread was retrieved, a section of the capillary tube was shattered every 30 seconds. The time it took to obtain the thread was called the clotting time.

2.5.8 Platelets

3.98 milliliters of platelet diluting fluid, also known as Rees-Ecker Fluid, should be placed in a dry, clean, and grease-free test tube. Add 20 µl or 0.02 ml of Blood Specimen (1:200 Dilution) with a micropipette to the tube containing the diluting fluid. After a few minutes of vigorous mixing, get your hemocytometer and Neubauer's Chamber ready.

$$\text{Total platelet count} = N \times \text{Dilution} / \text{Area} \times \text{Depth } N \times 20 / (1/5 \times 0.1).$$

$$\text{Total number of platelets} = N \times 1000 / mm^3$$

2.5.9 Urine Analysis

After the urine sample was obtained in a test tube and 10ul was placed to the urine analysis strip (Acon), it was analyzed by two independent observers.

3. RESULTS

3.1 Improvement of the UV-Vis Spectroscopy Application of Silver Nanoparticle Biosynthesis

After adding the green leaf extract and letting the mixture sit in the light at room temperature, the reaction mixture's color changed from green to a colorless silver nitrate solution. As seen in Fig. 1a, the color of the reaction mixture turned brown. At 460 nm, the reaction mixture's maximum absorbance was recorded.

3.2 SEM Assessment

A well-defined, spherical, aggregation-free silver nanoparticle (Fig. 1) was discovered via scanning electron microscopy. With the use of a scanning electron microscope, the size and shape of the nanoparticles were examined (Nova Nano SEM 450, USA).

3.3 TEM Assessment

TEM images of the generated silver nanoparticles were captured at different magnifications. The findings show that the nearly spherical green nanoparticles made via biosynthesis have a size range of 10 to 50 nm (Fig. 2).

3.4 Schematic for XRD

The polycrystalline nature of AgNPs was confirmed by the XRD pattern analysis (Fig. 3). The XRD spectrum showed four prominent diffraction peaks at 2θ values of 38.18°, 44.25°, 64.25°, and 77.40°. These numbers matched values indexed at the (111), (200), (220), and (311) lattice planes. Bragg's reflections of the face-centered cubic (FCC) structure of metallic silver. The XRD examination confirmed the identity of the resultant particles as silver nanoparticles. The broad and noticeable spectrum peaks of silver nanoparticles reveal their small particle size and crystalline structure.

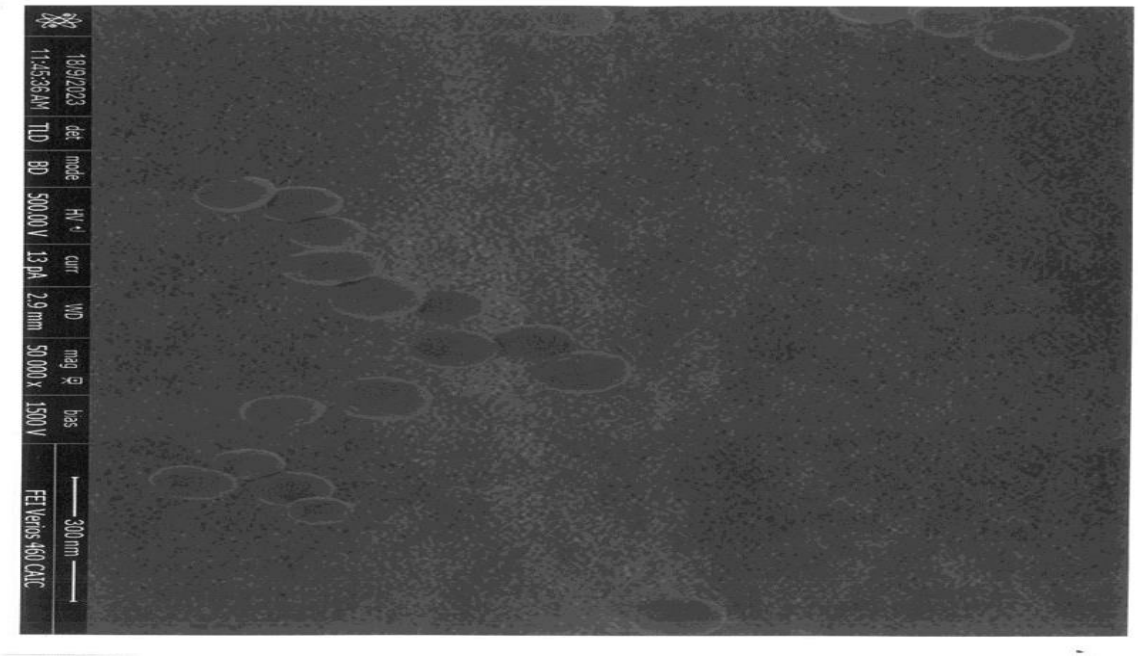

Fig 1: SEM analysis of biosynthesized silver nanoparticles a SEM image of synthesized nanoparticlesMurrayaKoenigiiAg NPs

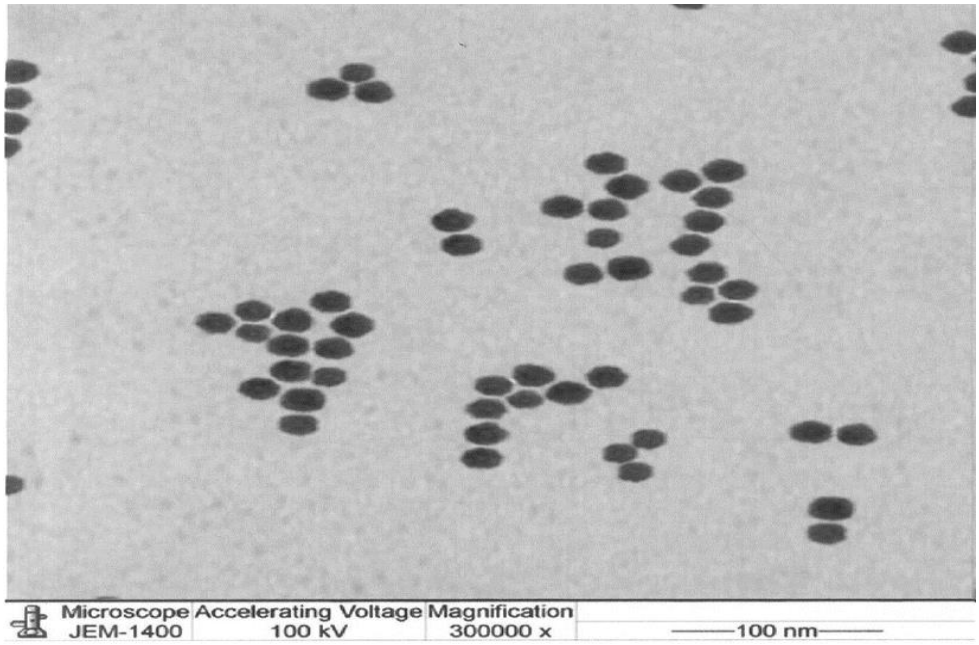

Fig 2: Topographical image of colloid silver nanoparticle from TEM analysis a–c under diferent magnification MurrayaKoenigiiAgNPs

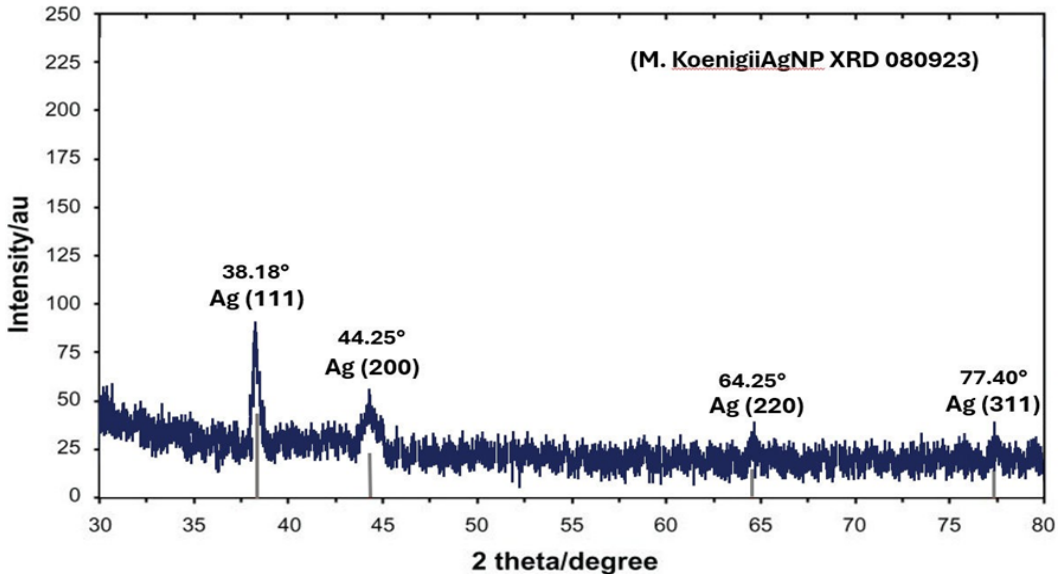

Fig 3: X-ray diffraction pattern of silver nanoparticle prepared with aqueous leaf extract of MurrayaKoenigii AgNPs

3.5 FTIR Examination

Figure 5 illustrates the FTIR spectra of the silver nanoparticles biosynthesised and the leaf extract. The peaks observed in the leaf extract FTIR spectrum (Figure 5) were as follows: 3454.89, 3394.96, 3285.57, 2920.82, 2855.61, 2382.04, 2312.32, 2103.68, 1557.39, 14210.31, 1050.33, 610.02, and 529.64 cm-1. The leaf extract exhibited absorption peaks within the range of 4000–3000 cm−1 (specifically, 3454.89, 3394.96, and 3285.57 cm−1). These peaks indicated the presence of an O–H stretching hydroxyl functional group, which could be in a free state or formed strong hydrogen bonds. The presence of phytoconstituents, including flavonoids, polyphenols, and tannins, is indicated by these peaks. The presence of C–H stretching alkanes can be

inferred from the successive peaks (2920.82, 2855.61, 2382.04, 2312.32, and 2103.68cm−1) in the 3000–2000 cm−1 wavelength range. Within the range of 2000–1000 cm−1, the highest wave numbers recorded were 1724.28, 1557.39, 1420.01, and 1050.33 cm−1. The findings of this study indicate the presence of C=O, C=N, C=C, O–H, and C–H elongation, which may indicate the existence of glycosides, tannins, and triterpenes. The peaks observed at 677.34, 610.02, and 529.64 cm-1 within the range of 1000–500 cm−1 are indicative of O–C and alkyl halide (C–X) stretching, respectively. It illustrates the coexistence of acidic constituents and meta-aromatic hydrocarbons. As suggested by the absence of peaks in the FTIR of the nanoparticles, the polyphenolic components present in the extract, which correspond to the H-bond, OH stretch, and C-H stretch, may be significant in the reduction and capping of silver ions and C-H stretch, both of which potentially contribute significantly to silver ion reduction and capping.

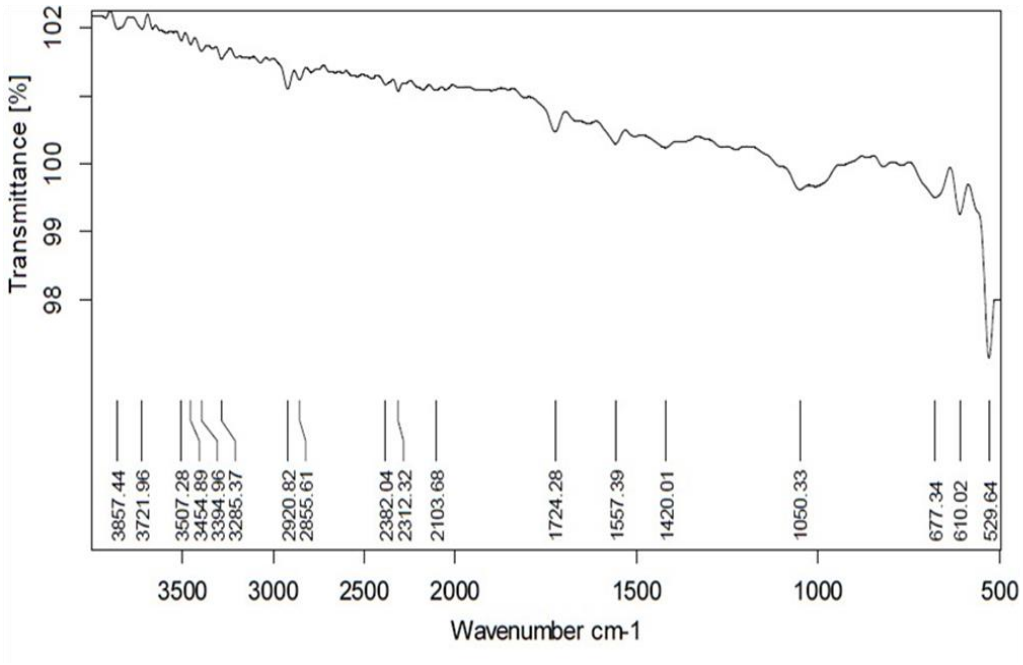

Fig 4: FTIR Spectra *MurrayaKoenigii*AgNPs

Table 4: In-vivo antidiabetic activity of silver nanoparticle and leaf extract of M. Koenigii L. percentage (mean±SE)

Name of sample	Results (Blood Glucose mg/dl)
Uninduced Untreated	77.404 ± 2.89
Induced Untreated	333.14 ± 8.50
M. Koenigii Ext	268.28 ± 1.81
M. KoenigiiAgNPs	241.97 ± 2.75
Gilbenclamide	141.71 ± 7.05

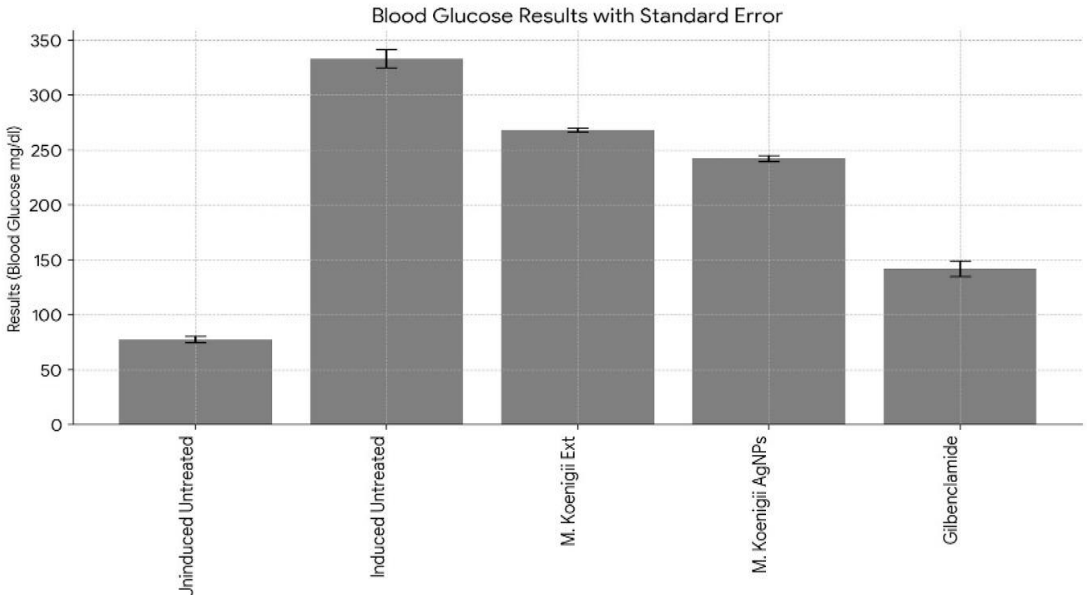

Fig 9: In-vivo antidiabetic activity of silver nanoparticle and leaf extract of M. Koenigii L.

Table 5: Comparison of Body Measurement between Uninduced Untreated and MurrayaKoenigiiAgNps, percentage (mean±SE)

Sample	Body wt.	WBC 103/mm3	RBC (106/ul)	Hb (gm/dl)	CLOTTING	PLATELET	SGOT IU/L	SGPT U	Urobilinogeu mol/l
Uninduced Untreated	143.68 ± 3.66	7.71 ± 0.23	6.336± 0.05	10.07± 2.43	96 ± 6.00	273.8 ± 21.14	107.76 ± 1.56	126.42 ± 1.04	11.6 ± 3.30
M. KoenigiiAg NPs	140.54 ± 3.07	7.74 ± 0.19	6.29 ± 0.06	12.60 ± 0.14	96.00 ± 6.00	304.00 ± 24.01	110.60 ± 3.8	126.62 ± 0.80	11.60 ± 3.30

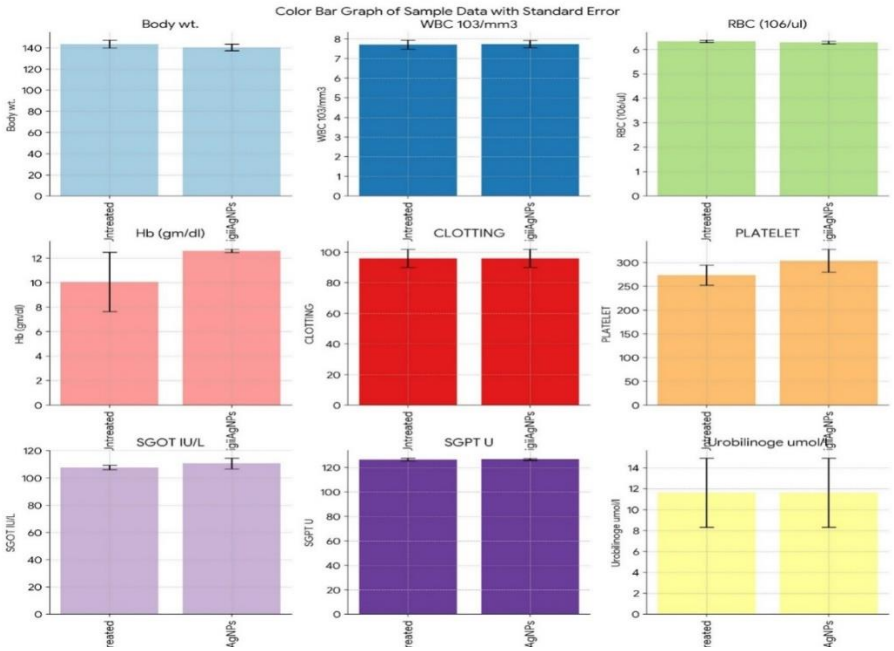

Fig 10: Comparison of Body Measurement between Uninduced Untreated and MurrayaKoenigii AgNps

Table 6: Comparison of Blood Parameters in Urine. percentage (mean±SE)

Sample	Bilirubin umol/l	Ketone mmol/l	Protein g/l	Nitrite	Leukocytes	Glucose	Specific Gravity	pH	Blood In Urine
Uninduced Untreated	31.4 ± 3.60	0.7 ± 0.20	0.27 ± 0.03	Negative	26 ± 11.00	5 ± 0	1.007 ± 0	6 ± 0	Absent
MurrayaKoenigiiAgNPs	31.40 ± 3.6	0.90 ± 0.24	0.27 ± 0.03	Negative	26.00 ± 11.00	5.00 ± 0	1.01 ± 0	6 ± 0	Absent

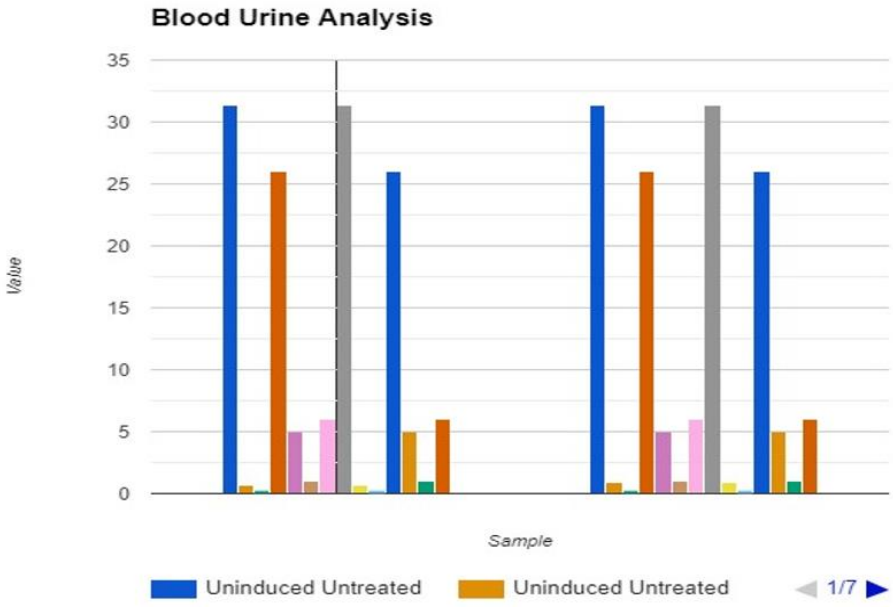

Fig 11: Comparison of Blood Parameters in Urine

4. DISCUSSION

Numerous metal-based nanoparticles are produced via the use of physicochemical processes [27]. The use of nanoparticles in medicine has expanded steadily [28]. Drug-loaded nanoparticles were easily absorbed deep within the affected tissues and organs [29]. The need for green nanoparticle production has increased since it has less of an impact on the environment. It was swiftly and in great quantities, always the same size. Plant extracts were successfully used to produce nanoparticles in an eco-friendly manner [30]. These extracts help lower metal ions and are involved in capping. A function of the extract's secondary metabolites with unique functional groups is to stabilize and convert Ag+ to Ag0 during the green route-based manufacturing of silver nanoparticles. One practical technique for keeping an eye on the creation of nanoparticles is UV-Vis spectroscopy. It is widely used to confirm how silver nanoparticles are made. As soon as the addition of MurrayaKoenigii leaf extract caused a noticeable change in the color of the silver nitrate solution, turning it from green to brown. The absorbance of the reaction mixture peaked at 460 nm. This color shift was explained by the surface plasmon response phenomenon, which demonstrated that silver nitrate was converted to silver ions (Ag+) [5]. It offers details

on the biological synthesis of silver nanoparticles. The highest absorption in the 400–460 nm range tells us something about how silver nanoparticles are made. Several papers have shown silver nanoparticle absorption at this wavelength [1]. A number of variables, including extract concentration, silver nitrate content, and duration of light exposure, are important in determining how quickly, effectively, and of high quality silver nanoparticles may be synthesized. In previous studies, these components were evaluated for the environmentally friendly synthesis of silver nanoparticles [31]. The UV-Vis spectra clearly showed that spherical silver nanoparticles underwent a sharp SPR band formation [32]. The size of the silver nanoparticle that was formed depended on the concentration of silver nitrate. The size of the particles increased with the concentration of silver nitrate [33]. By adjusting the reaction time and different leaf extract concentrations, the size of the produced silver nanoparticle may be regulated. The UV-Vis spectrum revealed that increasing the reaction time length led to a higher concentration of spherical silver nanoparticles forming, which produced a sharper, higher-intensity SPR band [32]. The size of the generated nanoparticle is determined by the concentration of silver nitrate. The size of the particles increased with the concentration of silver nitrate [33]. Numerous techniques, including TEM, SEM, XRD, and FTIR analysis, were used to describe the AgNPs. The size and form of the nanoparticles were ascertained by TEM analysis. Phosphate level monitoring can provide insight into the body's acid-base balance, which is affected by the effects of anti-diabetic drugs as well as metabolic changes associated with diabetes. In summary, these measures facilitate understanding of how antioxidant and anti-diabetic therapies affect a variety of physiological processes, including inflammation, metabolic changes, liver and kidney function, and continence. A complete evaluation of the treatment's safety and efficacy can be accomplished by monitoring these metrics. [34] The artificially generated nanoparticles considerably decreased the mice's fasting glucose levels and enhanced their insulin sensitivity and glucose tolerance.

5. CONCLUSION

This study's primary goal was to produce a green-route nanodrug for diabetes that would be less likely to cause side effects and be safer and more biocompatible than synthetic medications. An aqueous extract rich in bioactive chemicals from the medicinal plant "MurrayaKoenigii" was used as a capping agent to stabilize the nanoparticles after it was synthesized as a reducing agent. The characterisation of the newly biosynthesized silver nanoparticles was confirmed using techniques like FTIR, XRD, TEM, and SEM. The presence of polyphenols and favonoids in the leaf extract is what causes its antidiabetic characteristics. With the help of sunshine, aqueous leaf extract was able to efficiently produce silver nanoparticles. The resulting spherical, polycrystaline nanoparticles have an absorption spectra measured using a range of techniques at 460 nm. They were between 10 and 50 nm in size. The antidiabetic action of silver nanoparticles on tested diabetics demonstrates their efficacy as antidiabetic agents and opens up new avenues for the creation of simple, affordable drugs. The antidiabetic potential of MurrayaKoenigii is also supported by a number of other parameters, including bilirubin umol/l, ketone mmol/l, protein g/l, nitrite, leukocytes, glucose, specific gravity, pH, blood in urine, body weight, WBC 103/mm3, RBC (106/ul), hemoglobin (gm/dl), clotting platelets, SGOT IU/L, and SGPT Urobilinogen umol/l. The current work may significantly contribute to the development of environmentally friendly synthetic nanoparticles as antidiabetic agents. We get to

the conclusion that the artificial nanoparticles have a greater ability to lower hyperglycemias, which promote insulin sensitivity and glucose absorption. According to our findings, silver nanoparticles may be able to selectively restore the cellular morphology of the pancreas, liver, and kidney. Nevertheless, additional investigation is required to validate these results.

Compliance with Ethical Standards

Conflict of interest: All authors declare that they have no conflict of interest**.**

References

1) Dixon, J.B.; Zimmet, P.; Alberti, K.G.; Rubino, F. Bariatric surgery: An IDF statement for obese type 2 diabetes. Surg. Obes. Relat. Dis. 2011, 7, 433–447.

2) Brownlee, M. The pathobiology of diabetic complications: A unifying mechanism. Diabetes 2005, 54, 1615–1625.

3) Marín-Peñalver, J.J.; Martín-Timón, I.; Sevillano-Collantes, C.; del Cañizo-Gómez, F.J. Update on the treatment of type 2 diabetes mellitus. World J. Diabetes 2016, 7, 354.

4) Pradhan, A.D.; Manson, J.E.; Rifai, N.; Buring, J.E.; Ridker, P.M. C-reactive protein, interleukin 6, and risk of developing type 2 diabetes mellitus. JAMA 2001, 286, 327–334.

5) National Diabetes Data Group. Classification and diagnosis of diabetes mellitus and other categories of glucose intolerance. Diabetes 1979, 28, 1039–1057.

6) AK Dash, J Mishra, DK Dash : Antidiabetic activity and modulation of antioxidant status by Ocimum canum in streptozotocin-induced diabetic rats; European Scientific Journal, Volume,10,issue-6(2014)

7) Steyn, N.P.; Mann, J.; Bennett, P.H.; Temple, N.; Zimmet, P.; Tuomilehto, J.; Lindström, J.; Louheranta, A. Diet, nutrition and the prevention of type 2 diabetes. Public Health Nutr. 2004, 7, 147–165.

8) 8.Jackson, R.A.; Hawa, M.I.; Jaspan, J.B.; Sim, B.M.; DiSilvio, L.; Featherbe, D.; Kurtz, A.B. Mechanism of metformin action in non-insulin-dependent diabetes. Diabetes 1987, 36, 632–640.

9) M. Jeyaraj, G. Sathishkumar, G. Sivanandhan, A.D. Mubarak, M. Rajesh, R. Arun et al., Colloids Surf. B 106, 86–92 (2013)

10) N. HanumantaRao, N. Lakshmidevi, S.V.N. Pammi, P. Kollu, S. Ganapaty, P. Lakshmi, Mater. Sci. Eng. C 62, 553–557 (2016)

11) J Mishra, AK Dash, DK Dash - Nature's Drug Store: The Free Tree of India; World Journal of Pharmacy and Pharmaceutical,volume-2, 4778-98(2013)

12) Mandal S, Vishvakarma P. Nanoemulgel: A Smarter Topical Lipidic Emulsion-based Nanocarrier. Indian J of Pharmaceutical Education and Research. 2023;57(3s):s481-s498.

13) Mandal S, Jaiswal DV, Shiva K. A review on marketed Carica papaya leaf extract (CPLE) supplements for the treatment of dengue fever with thrombocytopenia and its drawback. International Journal of Pharmaceutical Research. 2020 Jul;12(3).

14) Mandal S, Bhumika K, Kumar M, Hak J, Vishvakarma P, Sharma UK. A Novel Approach on Micro Sponges Drug Delivery System: Method of Preparations, Application, and its Future Prospective. Indian J of Pharmaceutical Education and Research. 2024;58(1):45-63.

15) Mishra, N., Alagusundaram, M., Sinha, A., Jain, A. V., Kenia, H., Mandal, S., & Sharma, M. (2024). Analytical Method, Development and Validation for Evaluating Repaglinide Efficacy in Type Ii Diabetes Mellitus Management: a Pharmaceutical Perspective. *Community Practitioner*, *21*(2), 29–37. https://doi.org/10.5281/zenodo.10642768

16) Singh, M., Aparna, T. N., Vasanthi, S., Mandal, S., Nemade, L. S., Bali, S., & Kar, N. R. (2024). Enhancement and Evaluation of Soursop (Annona Muricata L.) Leaf Extract in Nanoemulgel: a Comprehensive Study Investigating Its Optimized Formulation and Anti-Acne Potential Against Propionibacterium Acnes, Staphylococcus Aureus, and Staphylococcus Epidermidis Bacteria. *Community Practitioner*, *21*(1), 102–115. https://doi.org/10.5281/zenodo.10570746

17) Khalilullah, H., Balan, P., Jain, A. V., & Mandal, S. (n.d.). *Eupatorıum Rebaudıanum Bertonı (Stevıa): Investıgatıng Its Antı-Inflammatory Potentıal Vıa Cyclooxygenase And Lıpooxygenase Enzyme Inhıbıtıon - A Comprehensıve Molecular Dockıng And Admet*. *21*(03), 118–128. https://doi.org/10.5281/zenodo.10811642

18) Mandal, S. (n.d.). *Gentamıcın Sulphate Based Ophthalmıc Nanoemulgel : Formulatıon And Evaluatıon , Unravellıng A Paradıgm Shıft In Novel Pharmaceutıcal Delıvery Systems*. *21*(03). https://doi.org/10.5281/zenodo.10811540

19) Mandal, S., Tyagi, P., Jain, A. V., & Yadav, P. (n.d.). *Advanced Formulation and Comprehensive Pharmacological Evaluation of a Novel Topical Drug Delivery System for the Management and Therapeutic Intervention of Tinea Cruris (Jock Itch)*. *71*(03). https://doi.org/10.5281/zenodo.10811676

20) J Mishra, AK Dash, R Kumar ; Nanotechnology Challenges; Nanomedicine: Nanorobots International Research Journal of Pharmaceuticals, Volume,2 Issue 4 (2012)

21) Ahmad A, Senapati S, Khan MI, Kumar R, Ramani R, Srinivas V, Sastry M. Intracellular synthesis of gold nanoparticles by a novel alkalotolerant actinomycete, Rhodococcus species. Nanotechnology. 2003 Jun 6;14(7): 824.

22) Shakti Jaiswal, Alok Kumar Dash,,Jhansee Mishra. Development and characterization of a novel nano-liposomal formulation of famotidine-loaded nano-sized liposomal with biodegradable polymer. Bull. Env. Pharmacol. Life Sci., Vol 12[6] May 2023: 82-91.

23) Das S, Sharangi AB. Madagascar periwinkle (Catharanthus roseus L.): Diverse medicinal and therapeutic benefits to humankind. Journal of Pharmacognosy and Phytochemistry. 2017; 6(5): 1695-701.

24) A.W. Bauer, W.M.M. Kirby, J.C. Serris, M. Turck, Am. J. Clin. Pathol. 45, 493–496 (1966)

25) W. Williams Brand, M.E. Cuvelier, C. Berset, LWT Food Sci. Technol. 28, 25–30 (1995)

26) S. Iravani, H. Korbekandi, S.V. Mirmohammadi, B. Zolfaghari, Res. Pharm. Sci. 9, 385–406 (2014)

27) W.H. DeJong, P.J.A. Borm, Int. J. Nanomed. 3, 133–149 (2008)

28) C. Saraiva, C. Praça, R. Ferreira, T. Santos, L. Ferreira, L. Bernardino, J. Control. Release 235, 34–47 (2016)

29) DA Kumar, S Dharmendra, M Jhansee, N Shrikant: Development and characterization of chitosan nanoparticles loaded with amoxicillin; Int Res J Pharmacy, Volume – 2;(2011)

30) V. Manikandan, P. Velmurugan, J.H. Park, W.S. Chang, Y.J. Park, P. Jayanthi et al., 3 Biotech 7, 72 (2017)

31) H. Bar, D.K. Bhui, G.P. Sahoo, P. Sarkar, S.P. De, A. Misra, Colloids Surf. A 339, 134–139 (2009)

32) AK Dash, J Mishra ; Formulation and in vitro characterization of chitosannanoparticles loaded with ciprofloxacin hydrochloride; Der Pharmacia Lettre, Volume-5,Issue-4,126-131(2013)

33) S.M. Roopan, G. Madhumitha, A. Abdul Rahuman, C. Kamaraj, A. Bharathi, T.V. Surendra, Ind. Crop. Prod. 43, 631–635 (2013)